LASER INTERFEROMETER GRAVITATIONAL WAVE OBSERVATORY
- LIGO -
CALIFORNIA INSTITUTE OF TECHNOLOGY
MASSACHUSETTS INSTITUTE OF TECHNOLOGY

Technical Note	**LIGO-T1600123-v1**	2016/08/31

Final Report - SURF 2016

R.Maggiore
Mentors:
X.Ni
G.Vajente

Distribution of this document:

LIGO Scientific Collaboration

Draft

California Institute of Technology
LIGO Project, MS 18-34
Pasadena, CA 91125
Phone (626) 395-2129
Fax (626) 304-9834
E-mail: info@ligo.caltech.edu

Massachusetts Institute of Technology
LIGO Project, Room NW17-161
Cambridge, MA 02139
Phone (617) 253-4824
Fax (617) 253-7014
E-mail: info@ligo.mit.edu

LIGO Hanford Observatory
Route 10, Mile Marker 2
Richland, WA 99352
Phone (509) 372-8106
Fax (509) 372-8137
E-mail: info@ligo.caltech.edu

LIGO Livingston Observatory
19100 LIGO Lane
Livingston, LA 70754
Phone (225) 686-3100
Fax (225) 686-7189
E-mail: info@ligo.caltech.edu

http://www.ligo.caltech.edu/

Abstract

The collective behavior of dislocations can lead to non-linear strain noise in metallic sample in response to slowly varying external stress field. Experiment and simulation on small-scale single crystalline system has suggested viscoplastic dislocation dynamics under low frequency stress modulation. This non-trivial mechanical noise that can propagate from the maraging steel suspension blades to the test mass is a potential up-conversion noise source for the gravitational wave detectors.
In order to directly apply the study in micro-nano scale to LIGO's concern, we want to input the developed micro-mechanical simulation results for the crackling noise form into the scaling model [2], and predict for the crackling noise progagated to the blade tip under prescribed loading.

1 Aim and Introduction

The Advance LIGO detectors are large-scale ground-based laser interferometers conceived for the detection of gravitational waves.
In this objective the displacement sensitivity that has to be reached is extremely high. In the working regime, for low frequency, the order of magnitude for the horizontal movement of the $40Kg$ fused silica mirror test masses must be $10^{-19}m/\sqrt{Hz}$.
In $Fig.1$ it is shown the scheme for the Advanced LIGO test mass suspension system, realized as a quadruple pendulum system for horizontal isolation; three stages of maraging steel cantilever are intended for vertical isolation. Any kind of mechanical noise taking place in the suspension sistem (wires, cantilevers), expecially for the lower set of cantilevers spring, because of the less vertical isolation from the test masses, could propagate to those and be a noise source which could limit the interferometer sensitivity.

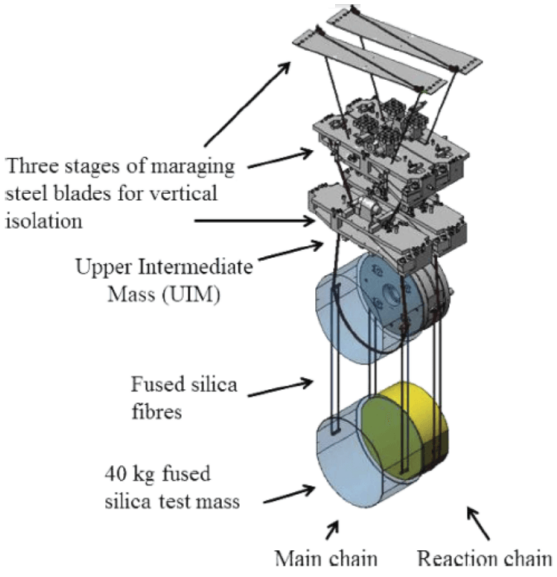

Figure 1: Scheme for the Advanced LIGO test mass suspension system, realized as a quadruple pendulum system for horizontal isolation; three stages of maraging steel cantilever are intended for vertical isolation.

As the result of the application of an external driving force metallic materials, as the ones used in the Advanced LIGO suspensions system, are elastically deformed for stresses whitin the yielding stress and the relation between stress and strain is linear; exceeding the yielding non-linear deviation occurs. Furthermore, from experimental investigations, dealing at the microscopic scale, is showed that metal deformations, due to the discreteness of the crystal lattice line defects, known as dislocations, and the discreteness of their motion as well, are not continuous but inhomegeneous in space and intemittent in time because of localized ob-

stacles. This phenomenon is studied as crackling noise for metals that are working in the plastic regime, where bursts are larger than the intrumental noise.
Advanced LIGO suspensions system is loaded within the macroscopically elastic regime. In this working regime we are interested in non-linear deviation, similar to those described above, that could be a source of up-converted noise from low frequency, mainly coming from residual sismic motion, into high frequency audio band.
First of all, to get a model to predict how the crackling noise progagates to the blade tip under prescribed loading, is necessary a micro-nano scale model as an "input function" for the macroscopic one. Due to the lackness of theoretical studies focused on non-linear deviation while metals are working on the elastic regime, we applied a model conceived for the plastic regime directly to the elastic. The first part of this work is a numerical simulation work focused on a parametric study where we have run several simulations at a time with varying parameters.
Completed the parametric study for the simulation and obtaining results that are close to the experimental observation, we implemented the crackling-noise-experiment [3] for the demodulation studies of the crackling noise.

1.1 Experimental Datas and Data Analysis

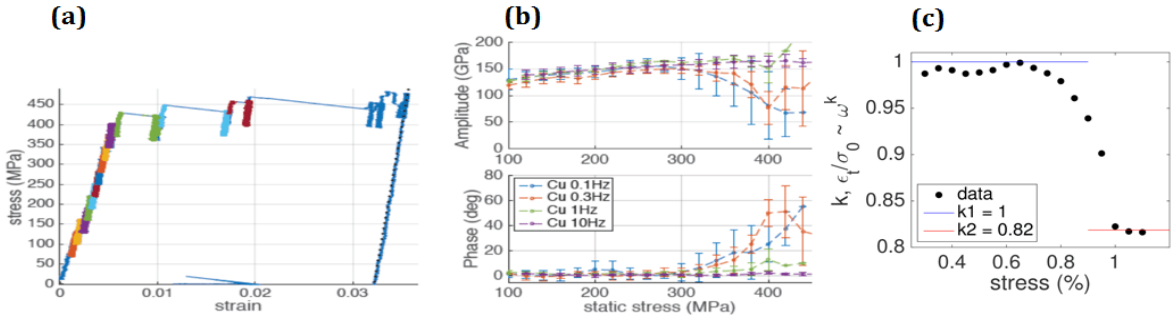

Figure 2: Micro-pillar (Copper, 500nm diamter, 400MPa nominal yielding stress) dinamic compression test experimental results[1].

In $Fig.(2)$ are plotted the results for the micro-nano scale experiment consisting in a micro-pillar (Copper, 500nm diamter, 400MPa nominal yielding stress) dinamic compression test [1]. A static load plus a sinusoidal driving force is applied to the copper micro-pillar; subsequently, the oscillation is turned-off, the static load increased and the oscillation turned on again. This process is iterated until a maximum stress fixed value that allow to explore all the working regimes for the pillar.

Data Analysis:

1. In $Fig.(2a)$ are plotted stress-datas versus strain-datas. Each colour stays for a different oscillation step.

2. Passing to the complex notation for stress, and strain:

   $\sigma(t) = Acos(\omega t) + iBsin(\omega t)$ - Stress
   $\varepsilon(t) = Ccos(\omega t) + iDsin(\omega t)$ - Strain

   and to define for a given time and pulsation:

   $H(\omega,t) = \frac{\sigma(\omega,t)}{\varepsilon(\omega,t)} = \tilde{H}e^{i\phi}$

   as our transfer function. With $\sigma(\omega,t)$ the Stress, $\varepsilon(\omega,t)$ the strain, and A,B,C,D are constant. If the system is living in the elastic regime $H(\omega,t)$ amplitude must be constant and phase zero, if they are not the system is not more elastic behaving.
   In $Fig.(2b)$ are plotted $H(\omega,t)$ amplitude(upper sub-graph) and phase(lower sub-graph) versus the static stress. Three regime can be distingusched:

   Elastic Regime: $(0, \sim 300)MPa$ - $\tilde{H} = Const$, $\phi = 0$ - Harmonic Oscillator;
   Micro-Plastic Regime:$(\sim 300, \sim 400)MPa$ - Transition phenomenon - First deviations of $\tilde{H}$ and ϕ, before nominal yielding;
   Plastic Regime: from $\sim 400MPa$ - Permanent phenomenon - Deviations and flatten out of $\tilde{H}$ and ϕ.

3. $Fig.(2c)$ is another quanitative way to fit the datas always using the complex notation.

   $\varepsilon(\omega,t) = \frac{\tilde{\sigma}}{\tilde{H}}e^{i(\omega t-\phi)}$
   $\varepsilon_t(\omega,t) = \frac{\tilde{\sigma}}{\tilde{H}}\omega e^{i(\omega t-\phi+\frac{\pi}{2})}$, the strain time rate

   and to define

   $\xi = \frac{|\varepsilon_t(\omega,t)|}{\tilde{\sigma}} = \frac{\omega}{\tilde{H}} \sim \omega^K$

   In our representation, $K_1 = 1.00$ stays for the linear regime, the system is elastic behaving; K_2 stays for the beginning of the plastic regime.

1.2 Theoretical Model and Methods

[5][4]

The theoretical model used to interpret our experimental datas considers the system on the mesoscopic scale and describes the dislocation motion through a disorder field of crystalline line defects, dislocations, under shear stress on a single slip plane.
The constitutive equation for the dislocation system:

$$\dot{\gamma}(r,t) = \frac{D}{\mu}\tau_{tot}(r,t) \tag{1}$$

Where r points the position on the slip plane, t is time, μ stays for the shear modulus, D is the diffusion rate and $\tau(r,t)$ represents the total stress which the dislocation is subjected.

And:

$$\tau_{tot}(r,t) = \tau_{ext}(t) + \tau_{int}(r) \tag{2}$$

$$\tau_{ext}(t) = T + Acos(\omega t) = T + Re\{\sigma(t)\} \tag{3}$$

$$\{\tau_{int}\}(\mathbf{k}) = -\frac{\mu}{[\pi(1-\nu)]}\gamma(\mathbf{k})\frac{k_x^2 k_y^2}{|\mathbf{k}|^4} = -C\gamma(\mathbf{k})\frac{k_x^2 k_y^2}{|\mathbf{k}|^4} \tag{4}$$

In $Eq.(3)$, $\tau_{ext}(t)$ is the external applied driving stress made by a static load T plus a sinusoidal part with a fixed amplitude A; it is considered space-indipendent.
In $Eq.(1)$, τ_{int} is the internal stress coming from the coupling interaction between dislocations; in $Eq.(3)$ it is expressed in the Fourier space. ν is the Poisson nuber and $\gamma(\mathbf{k})$ the strain.

The condition for the occurence of an avalanche, dislocation slipping, and meaning a deformation for our system is:

$$\tau_{ext}(t) + \tau_{int}(r) > \tau_{thr} \tag{5}$$

τ_{thr} is a threshold value randomly assigned. Physically, it represents the heterogeneites of the material properties. On mesoscopic scale, plastic deformation, may be spatially inhomogeneous.

Part I

Parametric Study

2 Parametric Study Results

Many simulations were carried out varying a single parameter to study the effects on simulation results.
The parameters, subjects, of this parametric study are:

Shape and Width of the Probability Distribution for Threshold Value; $Eq.(5)$

Elastic Coupling Coefficient - Varying:
C from $Eq.(4)$
D from $Eq.(1)$.

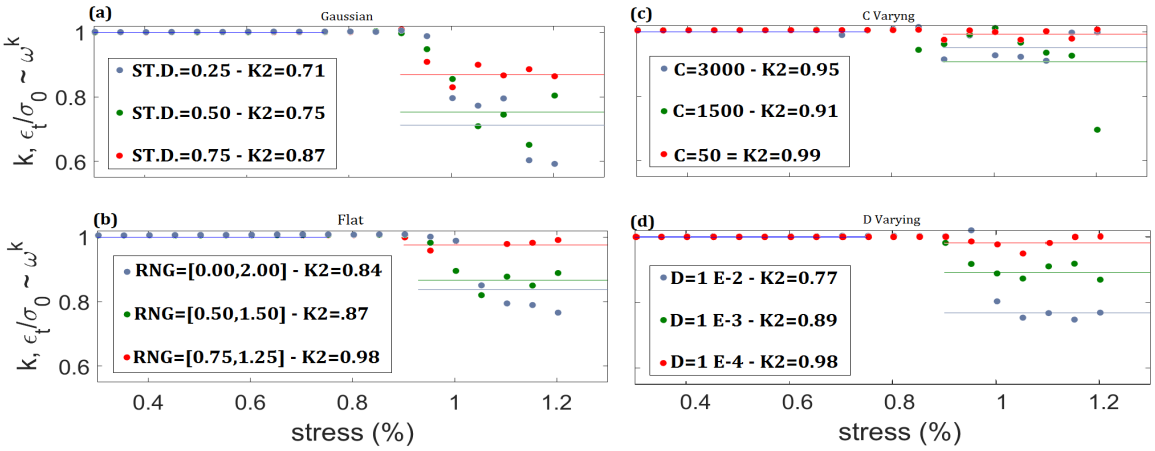

Figure 3: Parametric study simulation results. Data analysis is described in $Sec.(1.1)$.
(a) - Gaussian distribution for threshold value, $Eq.(5)$
(b) - Flat distribution for threshold value, $Eq.(5)$
(c) - C from $Eq.(4)$ varying
(d) - D from $Eq.(1)$ varying

2.1 Probability Distribution for Threshold Value - Shape and Width Varying

The elastic coupling coefficients were fixed to:

- $C = 400.00MPa$
- $D = (1.55 \cdot 10^{-6})1/s$

The choice seems reasonable because both values come from the non-updating threshold stress code [1] which fits the experimental data very well. Furthermore, we expected C would have been of the same order of magnitude of the nominal yielding point. D order of magnitude comes from previous check of the old code.
All the distributions used are centered in 1.0, definition for the yielding point in the simulations ($400.00MPa$). Fixed the elastic coupling coefficient and the distrbution shape width was varied. Expectancy was for a great sensibility for the micro-plasticity regime starting point to this parameter.

1. **Gaussian Distribution:**
   In $Fig.(3a)$ the results for increasing standard deviations are plotted and compared. In spite of all expectations, the micro-plasticity regime starting point seems not to depend on the width of the standard deviation. K average modulus amplitude is inversely proportional to the increasing of the standard deviation. Width increasing corresponds to the decrease of the average modulus amplitude. ($K_2 \propto \frac{1}{\sigma}$)

2. **Flat Distribution:**
   In $Fig.(3b)$ the results for increasing width for flat distribution are plotted and compared. The micro-plasticity starting point is not fixed, as in the Gaussian distribution, but it depends on the width of the distribution ρ. As for the Gaussian distribution, K average modulus amplitude is inversely proportional to the increasing of the distribution range ρ. Width increasing corresponds to the decrease of K average modulus amplitude. ($K_2 \propto \frac{1}{\rho}$)

Distribution width is a tuner for setting K average modulus amplitude; micro-plasticity regime starting point does not depend on distribution width.

2.2 Elastic Coupling Coefficient - Varying

Threshold distribution and, alternately, one of the elastic coupling coefficient were fixed to:

- Gaussian Distribution
- $D = (1.55 \cdot 10^{-6})1/s \Longrightarrow C$ Varying
- $C = 400.00MPa \Longrightarrow D$ Varying

The choice of a Gaussian distribution seems reasonable because it was the one used for the non-updating threshold stress code and it gaves a better data shape.

1. **C Varying**:
   In $Fig.(3c)$ the results for increasing C are plotted and compared. The micro-plasticity starting points inversely depends on the increasing of C. Constant increasing corresponds to a

negative shifting for the micro-plasticity regimes starting point, and viceversa, up to small C, where the regime is predominantly elastic. C is the tuner for the micro-plasticity regime starting point. K average modulus amplitude is sensitive to C varitions.

2. **D Varying**:
   In $Fig.(3d)$ the results for increasing D are plotted and compared. K average modulus amplitude is inversely proportional to the increasing of the distribution range. Constant increasing corresponds to the decrease of K average modulus amplitude, and viceversa, up to small D, where the regime is predominantly elastic. D is the other tuner, with the threshold distribution width, for setting K average modulus amplitude.($K_2 \propto \frac{1}{D}$)

2.3 Best Fitting

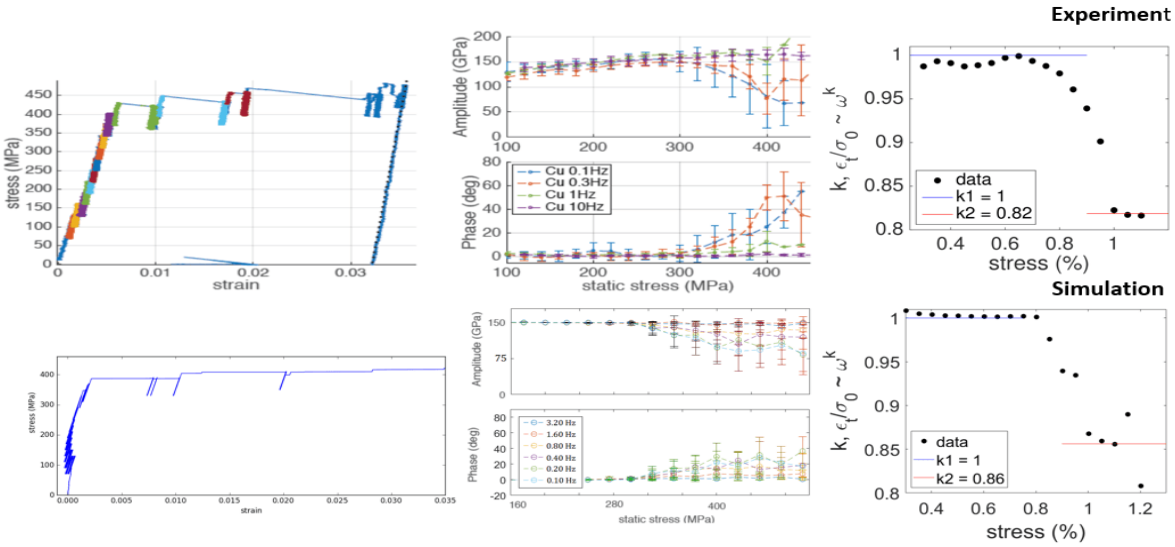

Figure 4: Simulation data best fitting to micro-pillar (Copper, 500nm diamter, 400MPa nominal yielding stress) dinamic compression test $Sec.(1.1)$ experimental datas[1]. Data analysis from $Sec.(1.1)$. Mean datas between 16 simulations for each frequency.
Simulation parameters:
Gaussian distribution $\sigma = 1$ - $C = 3000MPa$ - $D = (3.10 \cdot 10^{-4})1/s$.

- Gaussian Distribution - $\sigma = 1.00$
- $C = 3000.00MPa$
- $D = (3.10 \cdot 10^{-4})1/s$

It was used a Gaussian distribution for the above mentioned reasons ($Sec.2.1$)
To shift negativetly the micro-plasticity starting point C was fixed to $3000MPa$. To avoid K average modulus amplitude increasing, due to C increasing, D was fixed to $(3.10 \cdot 10^{-4})1/s$. Datas showed in $Fig.(4)$ are the mean between 16 simulaion for each frequency.

Part II

Crackling Experiment Simulations

3 Crackling Experiment Simulations Results

In the objective to excite up-conversion events a low frequency common driving force has been applied in to two micro-pillar, equal to the one described in $Sec.(1.1)$. To simulate the working regime of the Advanced LIGO suspension system, the common mode excitation has the form of $\tau_{ext}(t)' = T' + Acos(\omega t)$, a static load, $250MPa$ in our simulations, plus a sinusoidal part. The oscillation is periodically turned off and on in order to observe any kind of difference between the oscillation-on and oscillation-off datas and to establish if a demodulation analysis may be useful. In $Fig.(5)$, the signal datas are overlapped in one period driving.

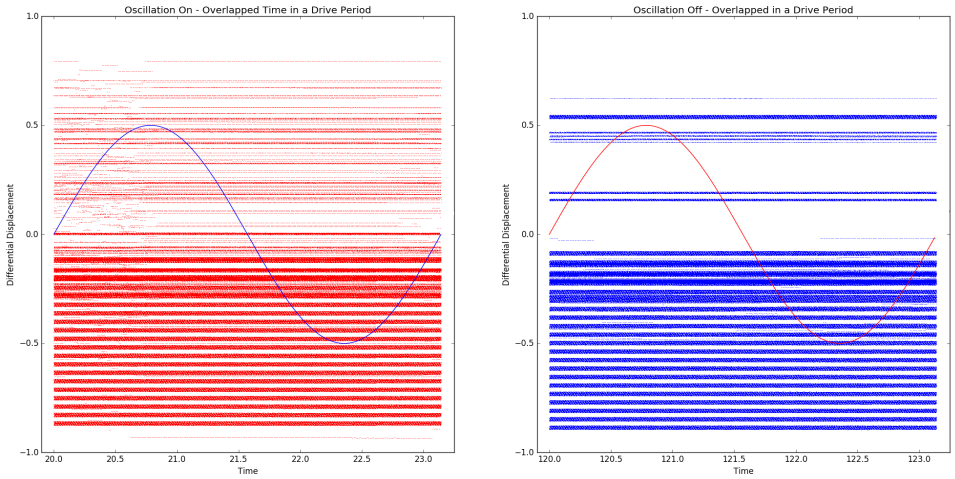

Figure 5: First crackling simulations results. Parameters of the simulations comes from the best fit got in $Sect.(2.3)$. On the left, in red, there are the datas for the turned on oscillation. On the right, in blue, there are the results for the turned off oscillation.

These are the preliminary results.
In order to implement the crackling-noise-experiment like loading condition and carry out different frequency and amplitude driving tests at constant nominal elastic stress, for the demodulation studies of the Crackling Noise, more simulations will be runned.

4 Future Work Planning

After finishing the parametric study for the simulation and obtaining results that are close to the experimental observation, we want to implement the crackling-noise-experiment like loading condition and carry out different frequency and amplitude driving tests at constant nominal elastic stress, for the demodulation studies of the Crackling Noise

In order to directly apply the study in micro-nano scale to LIGO's concern, we want to input the developed micro-mechanical simulation results for the crackling noise form into the scaling model [2], and predict for the crackling noise propagated to the blade tip under prescribed loading.

References

[1] X.Ni, "Micromechanical Investigation on Crackling Noise, Crackle Meet @Pasadena" (2016)

[2] G.Vajente, "Crackling Noise: Scaling Model", LIGO-T1600246-v2 (2016)

[3] G. Vajente, E. A. Quintero, X. Ni, K. Arai, E. K. Gustafson, N. A. Robertson, E. J. Sanchez, J. R. Greer, and R. X. Adhikari, "An instrument to measure mechanical up-conversion phenomena in metals in the elastic regime"(2016)

[4] S.Papanikolaou et. al., "Quasi-periodic events in crystal plasticity and the self-organized avalanche oscillator", Nature 490, 517522 (2012)

[5] M.Zaiser, "Scale invariance in plastic flow crystalline solids", Advance in Physics, 55:1-2, 185-245, DOI:10.1080/00018730600583514 (2006)